Sustainable Computing: Informatics and Systems 35 (2022) 100734

Contents lists available at ScienceDirect

Sustainable Computing: Informatics and Systems

journal homepage: www.elsevier.com/locate/suscom

An open platform for efficient drone-to-sensor wireless ranging and data harvesting

Tommaso Polonelli [a,*], Michele Magno [a], Vlad Niculescu [a], Luca Benini [a], David Boyle [b,*]

[a] ETH Zurich, Gloriastrasse 35, 8092, Zurich, Switzerland
[b] Imperial College London, Gloriastrasse 35, 8092, Zurich, United Kingdom

ARTICLE INFO

Keywords:
Drones
Wireless sensors
Ultra-wide band
Wake-up radio
Localization
Energy efficiency

ABSTRACT

Drones deployed in combination with wireless sensors can unlock a host of prospective applications in environments that lack infrastructure communications networks and where access may be impossible for human operators. Community building efforts to engage with this opportunity are hampered by a lack of platform support and an evolving understanding of the performance of known wireless communications systems in dynamic outdoor environments, particularly under mobility. This paper proposes and evaluates a new combination of ultra-wide band and wake-up radio technologies. These enable high precision landing and support energy efficient operation. We describe in detail the design and implementation of an open platform making use of the combination of these radios to improve upon ranging, bandwidth and energy efficiency problems that affect drone–wireless sensor systems. Our evaluation shows how established ideas including low power listening and receiver-initiated data transfer compare with using a wake-up radio. We show that the energy efficiency of the localization–acquisition cycle can be improved by up to 62% with respect to a duty cycle approach. Our experimental evaluation also shows two orders of magnitude improvements in power consumption, from 190 μW to 2 μW, in non-ranging quiescent states on the sensor side.

1. Introduction

The commercial unmanned aerial vehicle (UAV) or *drone* market is already worth ~$100B USD. This spans industries including infrastructure, agriculture, transport, security, media, insurance, telecommunications and mining [1,2]. As inexpensive drones proliferate, we are beginning to see their integration with terrestrial sensing devices and systems in many interesting ways, with recent examples including tracking first responders [3] and air quality monitoring [4]. Systems that integrate drones and terrestrial sensors have the potential to overcome many problems and challenges associated with deploying sensors in remote and inaccessible locations. Using drones as *mules* to gather data from sensing devices has been suggested by many researchers [5–8], and more recently as a means to recharge sensor devices [9–11]. There are many important application areas including security, precision agriculture and environmental monitoring, where the lack of infrastructure communications networks, insufficiently long sensor lifetime and challenging maintenance environments deter users from deploying wireless sensing devices [12].

Most experimental efforts reported in the literature make use of a patchwork of development kits (e.g. ultra-wide band (UWB)) and popular single board computers (e.g. Raspberry Pi) that are carried as the payload of an *off the shelf* drone, e.g. [3,8]. These tend to be *ad hoc*, with little community convergence around any particular platform. Converging around a small number of hardware and software platforms would almost certainly help to accelerate technical progress, lower the barrier to entry and broaden researcher engagement. In this work, we discuss the development of an open platform that enables integration with drones' on board SDKs and flight control software, in addition to multiple radios that we show can be used to improve localization accuracy and energy efficiency on both drone and sensor sides.

Although localizing devices may be a core part of an application in its own right, e.g. in [3], centimeter scale localization accuracy in outdoor environments is needed when the UAV is used to inductively recharge devices. While far field RF power transmission has been proposed for this purpose [13], near field inductive power transfer (IPT) offers much higher instantaneous power (tens to hundreds of watts) that enables rapid recharging of secondary energy buffers [9,11], but has a range of only tens of centimeters. Where devices are likely to be distributed across a large geographic area, we need solutions that exploit multiple wireless technologies to effectively locate and interact with sensors. One such approach incorporates using GPS to localize to within a number of meters before switching to UWB combined with

* Corresponding authors.
E-mail addresses: tommaso.polonelli@pbl.ee.ethz.ch (T. Polonelli), david.boyle@imperial.ac.uk (D. Boyle).

https://doi.org/10.1016/j.suscom.2022.100734
Received 26 March 2021; Received in revised form 15 February 2022; Accepted 29 March 2022
Available online 10 April 2022

altitude to further localize to within tens of centimeters [3,14,15]. This helps to overcome accuracy limitations associated with approaches like Time of Arrival (ToA), Received Signal Strength Indication (RSSI) and low power wireless radios (e.g. Bluetooth Low Energy or IEEE 802.15.4). Although state of the art GNSS localization technology can reach sub-meter accuracy using commercial products, sensitivity may be heavily affected by weather conditions, the number of satellites available in a given location, or hour of the day. Under these conditions, it is often impossible to guarantee centimeter landing/hovering precision. A single misalignment can cause an insufficient charge of the sensor node, which may become out of order and require human intervention to reboot. Assuming precise navigation using only satellites, as in our initial tests, the system will be dependent on land conditions, such as leaves, tall grass, and external intervention. For example, in one of our tests, animals shifted a sensor by a few meters. Even considering open environments and calm days, we found GPS to be reliably accurate to within a couple of meters, but still not sufficient for our mission profile.

Using drones as data mules and power delivery vehicles simultaneously creates an interesting trade-off in terms of proximity time between drone and sensor. In some cases, for example where a secondary cell may take ∼20 min to recharge, it may tolerable to accept a low bit rate. Considering devices powered by a supercapacitor (or small supercapacitor bank) that can charge in a matter of seconds, however, high throughput is important to minimize the total interaction time between drone and sensor. Under mobility in dynamic outdoor environments, achievable throughput using low power wireless radios is often only a fraction of the nominal rate [8,16]. Making use of the relatively higher throughput possible with UWB is thus desirable, which achieves 6 Mbps under realistic outdoor conditions. This is important for uploading larger time series sensor data from terrestrial devices and makes audio–visual data capture realistic.

Energy efficient operation of the terrestrial device is critical to minimize the maintenance schedule and prolong operational lifetime. Although energy performance on a per-bit basis is good (∼nJ/b), commercially available UWB modules consume power in the order of hundreds of mW when active and are not likely to be particularly suitable for long-lasting sensing applications without aggressive power management techniques, as used for communications [17,18]. We are thus motivated to ensure that the UWB radio is only active when absolutely necessary, i.e., briefly during ranging and data transfer. To maximize energy efficiency on the sensor side, we chose to explore the use of an *asynchronous* scheme implemented in hardware in the form of a wake-up radio circuit [19]. We show how this provides orders of magnitude power performance improvements compared with duty cycled approaches managed by software.

Performing repeatable experiments for combined drone–sensor platforms in outdoor environments is an area of concern. Unlike typical evaluations and experiments that would be performed across a number of well-known and established testbeds, almost all similar works are carried out in isolation. We believe that by creating an open platform and providing access to our raw traces, we can take a positive step in this direction. When using drones in combination with wireless sensors outdoors, challenges surrounding dynamic wireless channels are further exacerbated by mobility (speed and angle of approach for non-isotropic radiators, and potentially Doppler shift at low frequencies and high speeds) and weather conditions (wind, humidity), some insights into which are captured in our results. In summary, we propose and assess a new platform combining ultra-wide band and wake-up radio technologies to enable high-precision and energy efficient localization of sensors for emerging drone–sensor applications. Two different landing methodologies are proposed, comparing them in terms of average power consumption in sleep mode and average landing energy. Since the final landing protocol and methodology are not affected, in both cases we use ATWR, the landing precision is not affected. Our contributions include:

- A new multi-stage localization technique fusing GPS, UWB and asynchronous hardware enabled wake up trigger;
- Implementation and evaluation of the suitability of duty cycled UWB (low power listening mode) for drone–sensor applications;
- A proposed and evaluated asynchronous ranging protocol using WUR and UWB to minimize power consumption in sleep mode;
- In-field experimental evaluation of the energy consumption of both approaches;
- A new low-power sensor node design to exploit wireless power transfer (WPT) capabilities that is also capable of flight control on the drone side;
- Open source hardware and software,[1] in addition to a dataset containing all collected measurements during more than 60 experiments.

The remainder of this paper is organized as follows: Related Work is described in Section 2. Our proposed system architecture is described in Section 3. In Section 4 we explain the design of the new wireless sensor node, and provide detailed information about the WUR in Section 4.2. Section 5 details the UWB capabilities and performance characteristics under low power listening. Section 5.4 describes a new asynchronous approach used to wake the device using WUR. Experimental evaluation and assessment of our proposed platform are discussed in Section 6, showing the measurements collected and performance achieved under practical experimentation before concluding in Section 7.

2. Related work

Rapid developments in the area of intelligent autonomous vehicles over the past decade have seen their use extend to new fields, often in combination with other technologies to serve more complex purposes [20]. An emergent hot topic is to use UAVs to perform localization of nodes in WSNs [21], with further application to tracking first responders [3]. Knowing the precise location of a node, a UAV can fly to it for charging and data acquisition purposes [7,11]. While data collection using a wireless interface poses an interesting challenge (particularly considering speed of drone travel and wireless sensor orientation) [8], autonomous navigation to within a few centimeters for the purposes of highly efficient inductive power transfer between a UAV and a device has not yet been practically achieved.

UWB is a promising technology for localization because it can perform distance measurements with accuracy down to 10 cm [15,22]. Its main disadvantage, however, is its relatively high current consumption, i.e., up to 140 mA in receive mode [23]. Indeed, many of the off-the-shelf UWB products are mains-powered or have extremely limited battery lifetimes, for example in [24,25], where the battery lasts for only tens of minutes. On one hand, developing a localization system that can accurately estimate the position of fixed nodes can enable UAVs to fly to unexplored areas where they may need to find their way to distributed wireless sensors [17,21,26]. This mechanism can bring the drone relatively close to a sensor node to efficiently receive information, and with power transfer in mind, to recharge it [11]. Previous work also demonstrated the flexibility of UWB to achieve energy efficiency in an embedded system, without losing accuracy [15]. This paper focuses on using UWB with hardware-enabled asynchronous communication to achieve energy efficient wireless sensor operation in combination with UAVs. We provide the hardware design and algorithms that may be used in this way for a variety of application scenarios. In particular, where distance estimation may be performed by the drone using UWB with asynchronous mechanisms that allow the node to enable the radio transceiver only when the drone is close to it. This asynchronous duty-cycled UWB approach is under-explored. It is clear, however, that the energy performance achievable may still be

[1] https://github.com/tommasopolonelli/SynthSense-WSN-UAV.

relatively poor due to the high current draw in the listening mode. Thus, we posit WURs can play an important role in developing an energy-efficient localization system that incorporates UWB to deliver centimeter accuracy.

A Wake-Up Radio (WUR) is an *ad hoc* low power (μW) circuit that continuously listens for radio messages. WUR is studied and characterized by several papers in the literature, e.g., in [27], where the authors proposed a 1.3 μW RF receiver, in [28], where an integrated 98 nW IC implementation is presented, and finally, a 20 μW circuit with a sensitivity of −53 dBm developed by Le-Huy in [29].

The WUR scheme used in this work is a discrete circuit presented in [27]. On–off keying (OOK) is an amplitude modulation technique for representing digital data. In this way, a binary symbol 1 is communicated by transmitting a fixed-amplitude, fixed-frequency carrier wave for the duration of one bit. A binary symbol 0 is communicated by disabling the transmitter for the duration of one bit [30]. The WUR continuously listens to the transmission medium, which in this work is a transceiver capable of OOK message transmission. In our scenario, the OOK WUR transceiver is mounted on a drone, which establishes asynchronous communication with the sensor nodes deployed on the ground. The WUR uses addressing to request a response only from a particular node at a time, while the others remain dormant because they did not receive the proper wake-up message.

In contrast with previous works, e.g. [31], the goal of this paper is to combine and evaluate its utility as part of a UAV system comprising UWB for precision and low power landing algorithms. To the best of our knowledge, this is the first time a WUR is used in combination with ultra-wide band for these purposes. In addition, we propose algorithms that are able to both improve energy efficiency and provide UWB localization accuracy. Due to the capability of the WUR and power management, when an incoming message is detected, the WUR wakes the device, which in our case takes care of data transmission over the UWB interface while delivering an enormous energy saving [32] - reaching to three orders of magnitude.

In terms of application scenario, the combination between UWB and WUR is exploited to achieve an inductive power transfer (IPT) efficiency above 50%. To achieve this goal the coil misalignment must be low (e.g. below 25 cm), as tested and simulated by Aldhaher and Arteaga et al. in [33,34]. The proposed inductive power transfer systems operate at 13.56 MHz or 6.78 MHz and are capable of delivering several tens of watts instantaneously, where the coupling factor between the coils may be calculated as a function of separation and misalignment. The receiving circuit, comprised of a non-linear load, was also characterized in order to reflect different impedances to the transmitter at different tuning and couplings, and therefore represent the effects produced by changes in distance and variations between the drone and the sensor node.

It is worth highlighting some additional related research areas, in particular those concerning drone localization and navigation systems using visual means and/or wireless anchors, and those concerned with optimal path planning and joint optimization of path planning and communication [35]. Approaches like on-board visual inertial (VI) odometry-aided navigation, e.g. [36], are unsuitable for many application scenarios relevant to our work where the wireless devices required to be localized and charged blend into the scene or may be buried, for example. Scenarios where anchor or other devices are required to triangulate distance are also undesirable [37], as they impose a deployment criterion that mandates that a drone must be able to *see* more than one device simultaneously, akin to seeing multiple satellites for GPS, e.g. [38].

In the case of optimal path planning or joint optimization of propulsion and communication, e.g. [13,39], respectively, researchers are often forced to make inaccurate assumptions about communications ranges and effectiveness under different speeds, altitudes and approach vectors. We expect the proposed system and experimental results can help to inform the development of more accurate solutions to these problems, in addition to providing new contexts and opportunities for both accurate localization techniques and highly efficient communications.

Table 1
Sensors used by the onboard control framework.

Sensors	Working range (m)	Error (m)	Output
GPS	0–∞	10	3D coordinates
UWB	0.2–100	0.10	Distance scalar
Ultrasonic	0.2–7.5	0.01	Distance scalar

The max working range is determined by the implementation.

3. Proposed framework

In this section, we present an overview of the operating principle of the two-stage UAV system for wirelessly communicating and recharging sensor devices. The conceptual setup of the UAV, often referred to simply as the *drone*, and the overall system settings are described. Following this, we introduce the UAV's on-board control framework and the concept of multi-stage navigation.

3.1. Operating principle

The UAV is required to autonomously fly between its landing pad or base station and designated sensor nodes. The locations of the nodes likely to be known *a priori* with reference GPS coordinates. Upon arriving at a destination device, the drone is required to inductively charge the device's energy buffer (which may be a secondary battery or supercapacitor(s)), landing or hovering as close as possible to the IPT receiving coil. Meanwhile, the information stored (i.e. time series sensor data) in its internal memory are uploaded to the UAV using the high-speed UWB wireless link (∼6 Mbps). On completion of charging and data transfer, the drone moves to the next targeted node and repeats the above steps. The design of the optimal flight path and route optimization is an active research topic beyond the scope of this contribution, and hence is not discussed further.

The UAV has the master application role in our framework, enabling and disabling the communication with the sensor node, which has the UWB wireless interface (Section 5.1), sensing application, and IPT power management modules where relevant (Section 4). The IPT module of the UAV delivers power via appropriate power electronic circuitry (i.e. a class E/F rectifier in our case) and transmitting coil, directly connected to the main battery of the drone. A specific module manages the UAV attitude during all the flight manoeuvres such as take-off, hovering, cruise, and landing. The DJI M100 is the drone platform used in this work. The application layer has been designed from scratch and includes the on-board computer, the sensor data storage, and flight sensors. This layer provides various functionalities for the UAV to improve the localization accuracy fusing the GPS and UWB information, as well as the ultrasonic sensor.

3.2. Multi-stage navigation

The sensors used to control a UAV's approach to a static device are listed in . Using a standalone GPS navigation approach does not provide sufficient accuracy for the inductive power transfer specifications, which require a landing/hovering precision with a maximum lateral misalignment of ∼25 cm to keep the charging efficiency at or above 50%.

The drone uses several sensors to improve flight control accuracy, such as the UWB distance sensor, which has a wide range of operation and good accuracy, to within ∼10 cm. It works from 20 centimeters to approximately 100 m, where the upper bound depends on the transmitting power and the antenna's radiation pattern (not necessarily isotropic). According to the accuracy and the working range of the listed sensors, two stages of navigation are proposed. The first stage of the navigation needs only the GPS system, which guides the UAV from anywhere to a circular range of 10 meters from the desired location. During the first stage, the altitude could be a fixed safety level, but, at

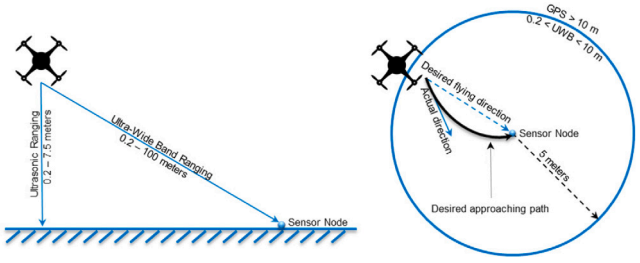

Fig. 1. Altitude component compensation for flying direction prediction using 2D gradient descendent.

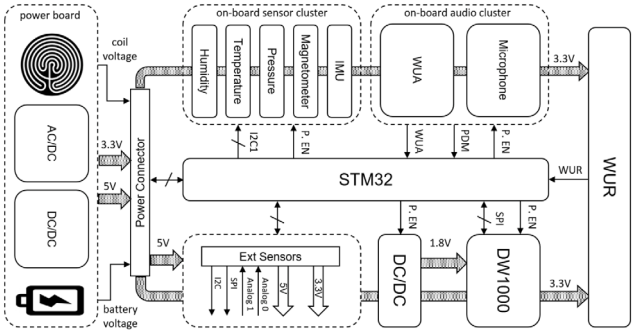

Fig. 2. Wireless sensor node schematic. The power connector splits the power electronics and the sensor boards.

the end of the first stage, a maximum altitude of a couple of meters, relative to the sensor position, should be adhered in order to prepare for the second stage. The second stage of the navigation starts from ∼10 m away from the sensor node's UWB antenna, receiving only the point-to-point scalar distance. To calculate a planar distance, a precise altitude value is required, and this is taken from the ultrasonic sensor.

The UWB distance estimation is utilized to compensate the GNSS error. A single UWB distance scalar measurement, however, cannot navigate the UAV to the actual sensor node location. A 2D gradient descendent algorithm is then introduced. It uses consecutive UWB measurements to adjust the flying direction, as shown in Fig. 1. To navigate in a horizontal plane and keep the height fixed, the ultrasonic sensor () is used for the height control and to remove the altitude component from the point to point distance, therefore obtaining a planar distance estimation (Fig. 1). The ultimate goal is to align the transmitting and the receiving coil, as they should be as close as possible (lateral misalignment of up to 25 cm) to reach the maximum battery charging efficiency [34].

The optimal landing curve that the UAV control applies in an ideal environment is described by Eq. (3). This is assumed to operate in the absence of wind, radio packet loss and measurement errors, and is valid for the last 100 meters before landing.

$$t_{\hat{d}} = \frac{\hat{d}}{|v|} \tag{1}$$

$$\sigma = \frac{1}{1 + e^{\frac{-(t_{land} - t_{\hat{d}})}{\rho}}} \tag{2}$$

$$v(t_{land}) = ((1-\sigma)\,|v|) + \left(\sigma\,|v|\, e^{(-(t_{land} - t_{\hat{d}})\frac{|v|}{\kappa})}\right) \tag{3}$$

where the UAV approaching speed ($|v|$) is 2 m/s, the maximum UWB working range is 100 meters () and it must be operative for the last 10 meters (κ) from the sensor node. $\hat{d}$ is a safety margin of 90 m to wake up the sensor node.

In Eq. (2), σ is the mathematical approximation of UAV control while switching between the GPS and UWB source. $t_{\hat{d}}$ (Eq. (1)) is the time that the drone needs to cover the $\hat{d}$ distance at $|v|$ speed. The corresponding t_{land} is used to calculate the drone's approach time, and is useful to estimate the average power consumption of the UWB radio on the sensor node side. For example, t_{land} is 71 s with a $|v|$ equal to 2 m/s.

4. Wireless sensor platform

4.1. Functional description

The sensor node in this work comprises three subsections. These are the sensor board, the power electronics board,[2] and the wake up radio receiver (WUR). The three boards are joined using two connectors, overviewed in Fig. 2. The power electronics board (PEB) deals with all tasks related to the power management, including generating reliable and stable 3.3 V and 5 V DC voltages from two Panasonic 18 650 batteries and managing the fast-charging and the wireless power transfer (WPT) that supports up to 150 W. The operating principle and characterization of the board are presented in [33,34]. For the scenario presented in this paper, the WPT system consists of two coils; a transmitting coil connected to the drone and a receiving coil incorporated into the PEB. A magnetic field, coupled with the receiver coil, is generated driving the transmitting coil with an alternate current, which induces a voltage across the PEB.

The sensor board features a multi-protocol radio front-end and many complementary sensors (locally and externally), to support a variety of sensor fusion and UAV applications (see Fig. 2). The PCB dimensions are 70 × 70 mm combined with the external UWB antenna of 30 × 40 mm. It supports the UWB compliant to IEEE 802.15.4-2011 for 2-way ranging and data transfer at rate up to 6.8 Mbps in addition to Bluetooth 5.0. The on-board STM32WB55RGV from STMicroelectronics manages all the stacks and the sensors. This MCU has the advantages of low energy design, as well as excellent peripherals support. ARM Cortex-M4 is used for the central processing tasks, while ARM Cortex-M0 is the radio communication protocols engine.

4.2. Wake up radio

In a typical sensor node, the radio transceiver is the most power-hungry component; therefore, the energy efficiency of the communication heavily impacts the average working time of these battery supplied devices. In previous works, such as [12,15,31], it has been demonstrated that aggressive duty cycling, turning the radio off and on periodically, significantly improves the lifetime of the network [40]. However, the duty cycling mechanism still has two side effects: the listening power consumption is not totally removed. Indeed, the transceiver needs to check the medium periodically with an intrinsic tradeoff between the latency and the power consumption.

In fact, the more the radio is powered off, the more energy is saved, but the latency will be higher. For this reason, asynchronous communication, which overcomes the latency/power trade-off, is considered one of the most efficient mechanisms for battery supplied sensor nodes [30]. In fact, with a WUR receiver, it is possible to decrease the idle-listening energy and achieve low latency communication, an essential factor in our framework where the drone needs to estimate the point-to-point distance in real-time. In this section, we present a brief introduction of both receiver and transmitter of the WUR structure, which is studied in-depth in our previous work [27,41].

[2] Although use is made of the PEB, it is not part of the open platform.

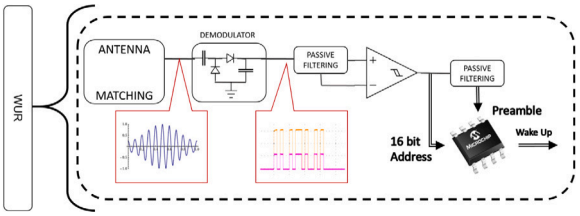

Fig. 3. Wake Up Radio: the receiver schematic in which is highlighted the envelope demodulator, the high-frequency low-pass filter, the comparator and, the MCU used to decode the address.

4.2.1. Receiver

Fig. 3 shows the architecture of the WUR circuit used in conjunction with the main sensor board. The receiver can decode only the OOK modulation, the simplest form of digital amplitude modulation in which each bit is represented as the presence or absence of a carrier wave. The WUR receiver architecture is made up of four main blocks: the 868 MHz matching network, the fully passive envelope detector, the comparator, and a μW MCU used to decode the address (Fig. 3).

Because WUR uses OOK modulation, the circuit consists of a passive envelope detector that discards the carrier frequency and its phase, only detecting the amplitude. We make use of a single-stage half-wave rectifier with series diodes, the $BAT15-04W$ RF Schottky diode pair from Infineon Technologies, which are optimized for frequencies up to 12 GHz. They offer a sensitivity of −56 dBm with the double diode schematic [42]. We selected the TLV3701CDBVT comparator from Texas Instruments for this work, which features a very low voltage offset of 250 μV and current consumption of 560 nA at 3.3 V. With this component, we can take advantage of the entire working range of the BAT15-04 W diode. To keep power consumption to a minimum, an 8-bit PIC12LF1552 was selected (20 nA in sleep mode). This also allows fast wake-up (∼130 μs at 8 MHz) and operating current of 30 μA/MHz, ∼30% lower than the STM32 W B55RG. When the PIC12LF1552 detects a valid address, it wakes up the STM32WB55RG through an interrupt pin (Fig. 3), which enables the DW1000 and the ATWR ranging protocol.

The average power consumption of the WUR receiver is 2 μW, which reaches 82 μW during the address decoding. Hence, for each reception the WUR needs 6 μJ considering a processing time of 24 ms (t_{beacon}).

4.2.2. Transmitter

The WUR transmitter aims to wake up the sensor node with as low latency as possible. It is, moreover, part of the drone payload and so must be lightweight. We use a simple 8-bit MCU, the PIC16LF1824T39 from Microchip that has been chosen for its current consumption in active mode, only 96 μA at 3 V and, 16.5 mA in transmission mode at 10 dBm. Usage of the WUR transmitter is straightforward. Once powered up, the PIC16LF1824T39 continuously streams the wake up packet with the destination address every 30 ms (P_{beacon}). The output power is 14 dBm. The transmission is done using 1 kbps data rate, using a beacon containing a 16-bit address and 8-bit preamble.

Considering the transmitter output power and receiver sensitivity, the communication link budget is 70 dB. To evaluate the effective functionality of the WUR in the proposed framework, we calculate the path loss with both free space and multi-path model, taking into account a worst-case scenario with a −5 dB gain antenna. In Fig. 4, simulations show that the minimum range required in our application is always covered, i.e. 10 m distance where the UWB ranging takes over from GPS. In particular, Est. Flath Earth Loss (Fig. 4) shows that the signal power goes below the WUR sensitivity after 10 m, while the free space model reaches this value over 40 m. These values are verified in Section 6.3, where in-field measurements are presented.

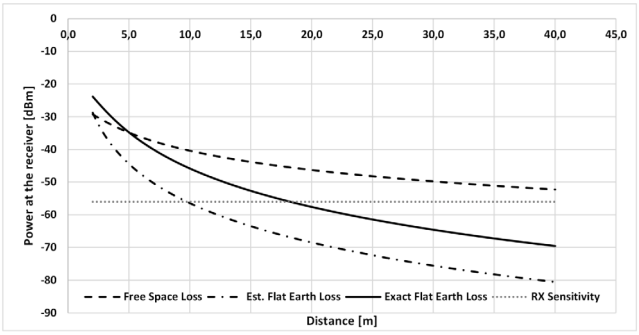

Fig. 4. Wake Up Radio: path loss calculation with free space and multi-path model. TX: 14 dBm, RX sensitivity: −56 dBm, Antenna Gain: −5 dB, Connector loss: −1 dB.

5. Ultra-wide band

This paper proposes a robust platform for UAVs and fully autonomous industrial applications in which environmental and generic external noise is compensated using complementary localization technologies. We have selected UWB for two reasons; a sensor node needs to transmit its data to a remote device; thus, this technology supports both high-speed and high-ranging precision, giving the best trade-off between cost and performance.

5.1. Decawave DW1000

We use the Decawave DW1000 [43], a low power radio transceiver compliant with IEEE 802.15.4-2011 standard. It is a System on Chip (SoC) embedding a wideband radio front-end. It contains a receiver, a transmitter, and a digital back-end. A serial digital bus interfaces the SoC to the host processor. The radio transceiver supports six bands between 3.5 GHz and 6.5 GHz with three selectable data rates: 110 kbps, 850 kbps and 6.8 Mbps. Our configurations use a carrier of 3.9936 GHz and a bandwidth (BW) of 499.2 MHz that corresponds to a 2 ns time width for the ultra-narrow electromagnetic impulse. A UWB message consists of binary symbols (i.e., bits), and a message typically starts with a preamble code that enables message detection by the other end [43].

We consider two possible configurations for the UWB module (i.e., DW1000) that are dynamically selected depending on the state of the system. First, there is *Configuration 1* which commands a pulse repetition (PRF) of 64 MHz and a preamble length of 1024. It involves a symbol rate of 110 kbps, and it is the adopted configuration for performing range measurements due to the high maximum operating distance associated with this data rate. Second, *Configuration 2* sets a PRF of 16 MHz and a preamble length of 128. This configuration is used after localization is performed and the drone is found nearby the node. Given the short distance between the drone and the node, broad coverage is not necessary anymore, and the 6.8 Mbps data rate adopted by *Configuration 2* leads to a faster transfer and, therefore, a lower energy consumption. The DW1000 has nine different power operation states: OFF, WAKEUP, INIT, IDLE, SLEEP, DEEPSLEEP, TX, RX, and SNOOZE. Detailed information is available in the DW1000's datasheet [43]. According to the datasheet of the UWB transceiver, it can also provide OOK messages that could, in theory, provide the wake-up for the WUR. Fig. 5 shows the measured power spectrum of the DW1000, where the maximum peak is around −35 dBm with an equivalent power spectral density of −110.8 dBm/Hz. Due to the poor gain within the operating frequency of the WUR (i.e., 868 MHz) and the sensitivity of the WUR, the resulting communication range is only 10 cm, however, which is clearly not sufficient for our target application.

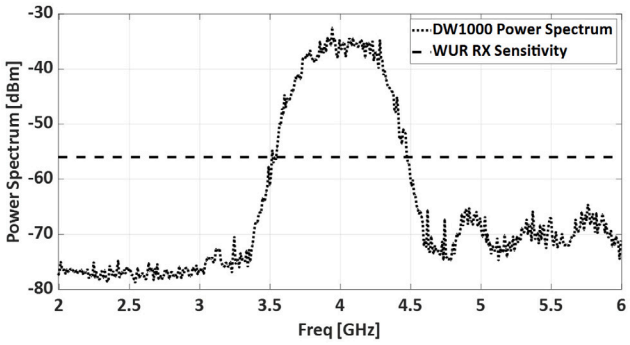

Fig. 5. DW1000 power spectrum with *Configuration 1*; the horizontal line highlights WUR receiver sensitivity.

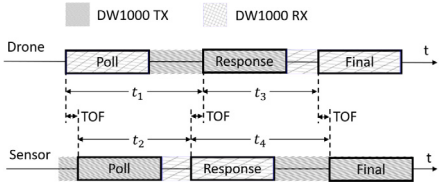

Fig. 6. Asymmetric double-sided two-way ranging (ATWR) method. Sequences of packets for ToF estimation.

5.2. Two-way ranging

The asymmetric double-sided two-way ranging (ATWR) protocol [44,45] is a scheme used by in Decawave SDK to calculate the distance between two DW1000s, further reducing the frequency drift rather than the standard two-way ranging estimation [43]. Indeed, the ATWR is considered asymmetric because it does not require equal reply times from each device. By the use of electronic and mathematical techniques to implement a clock with 15.65 ps precision, the DW1000 can determine the radio packet time of flight (ToF) using a threshold mechanism on the preamble chips. Using this method, the maximum error is in the low picosecond range, even with 20 ppm crystals, the worst-case specification [43]. The ATWR is fully supported by Decawave's SDK and is composed of three messages: Poll, Response, and Final. Each ATWR exchange consists of the drone sending the Poll message, the sensor node receiving the Response message, and then the node transmitting the Final message. The protocol sequence and the ToF formula is given in Fig. 6 and Eq. (4)

$$ToF = \frac{t_1 t_4 - t_2 t_3}{t_1 + t_2 + t_3 + t_4} \tag{4}$$

Since t_2 and t_3 have fixed and known values, 800 µs with an error of ±15.65 ps, from t_1 and t_4, the MCU calculates the round trip time as two times the ToF. One can note that the ranging scheme from Fig. 6 contains an odd number of UWB messages and therefore, if the drone initiates the communication, the sensor node will receive the last message and compute the UWB range. In order to communicate the range value to the drone, the node sends a fourth UWB message, called *optional message*. We assume that the ToF does not vary significantly between two consecutive messages withing an ATWR due to distance variation since the drone receives a delayed position estimation, this limits the maximum approaching speed of the drone to 3 m/s at the ranging frequency of 30 Hz. At this speed, the error generated is below the DW1000 uncertainty of ±5 cm [45]. This limitation is applied only for the last two meters, as when the distance between these two devices is above 2 m, ±5 cm precision is not mandatory. In our custom ATWR implementation, the Response packet includes two further fields besides standard values: the sensor battery and coil voltage, see Fig. 2. By interpreting the coil voltage, the UAV can infer if the two coils are aligned through a lookup table and it may precisely touch down [34].

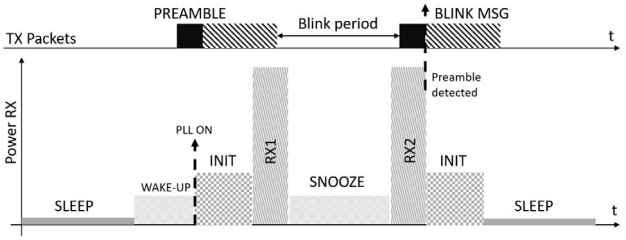

Fig. 7. DW1000 low power listen procedure. The DW1000 generates an interrupt if a preamble sequence is detected in RX1 or RX2.

5.3. ATWR optimization for energy efficiency

Concerning all DW1000 operation modes, the receiver operation is the highest in terms of power consumption. In *Configuration 1* and *Configuration 2* it draws from the battery respectively 81 mA ($I_{1,rx}$) and 122 mA ($I_{2,rx}$), almost two times the transmission current which is 50 mA ($I_{1,tx}$) and 69 mA ($I_{2,tx}$). On the other hand, the sensor board must continuously listen for radio signals from the drone. It is clear that a constant current of $I_{p,rx}$ is not sustainable for battery supplied sensor nodes, where the average current drawn should be lower than 9 mA to achieve one month of operation.

Aiming to increase the battery lifetime, we enable a unique low-power listening (LPL) feature on the DW1000 [43]. In low-power listening, the DW1000 is predominantly in the SLEEP state, waking up periodically for a short time. The DW1000 automatically returns to SLEEP for another period if no preamble is detected. The procedure is described in Fig. 7. Once a preamble is detected, the DW1000 reads the whole preamble and the data and signals the STM32 via an interrupt. The STM32 configures the DW1000 to continuous listening mode, enabling the ATWR ranging. To wake up the sensor node, the drone has to send the wake up message (i.e., Blink message) repeatedly for a long enough time so that the node receives it. However, in some corner cases, the on time of the node's UWB (i.e., RX1 in Fig. 7) may overlap with the data frame of the UWB packet and therefore it misses the preamble as shown in Fig. 7. To mitigate this issue and reduce the latency, the node's UWB is configured to switch on the receiver again (i.e., RX2), after a short sleep period that is defined as SNOOZE time in Fig. 7. This procedure is called *two-phase listening* and it ensures that if the first listening misses the preamble and hits the data frame of the message, the second listening window detects it. To minimize the ON-time of the node's UWB, we set the duration of two PAC intervals for both RX1 and RX2. The length of one PAC is configured to 32, which results in a duration of 96 µs for each of RX1 and RX2, given the data rate of 110 kbps of *Configuration 1*. This configuration results in a total time of 4.02 ms for the LPL, which includes also the INIT and SNOOZE time. Considering a duty cycle of 1%, we therefore need to use a total period of 402 ms, out of which 397.98 ms the node's UWB is found in SLEEP. Until the node wakes up, the Blink message is sent continuously, which contains a preamble of length 1024 and a data field of length 10. The total duration of one Blink message is 2.56 ms, where 1.1 ms are required to send the preamble. Therefore, we set a SNOOZE time of 2 ms, which is significantly larger than the time required to send the data frame of the Blink message. This ensures that at least one 'listen' (i.e., RX1 or RX2) will overlap with the preamble.

5.4. ATWR and WUR: an asynchronous approach

Compared to the previous section where we implement a duty-cycled approach, here we present the fusion of the UWB ATWR and WUR technology. The resulting radio protocol is straightforward: the sensor node is in deep-sleep mode with all the peripherals powered off. The only active components are the STM32WB55RGV's RTC and

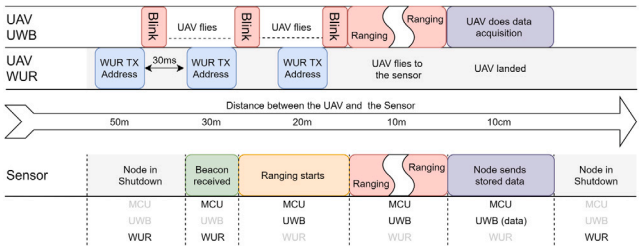

Fig. 8. Asynchronous ranging protocol. UWB and WUR fusion for low power and low latency distance estimation between UAVs and low power devices.

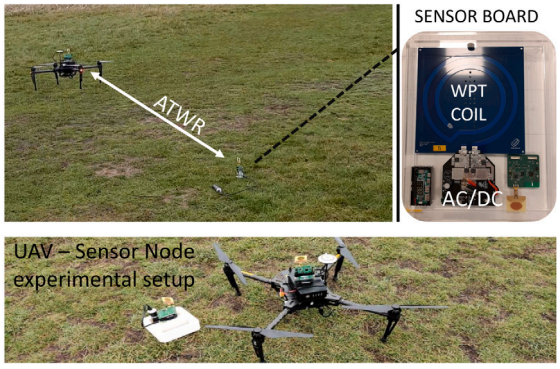

Fig. 9. Top: Drone approaching the sensor node using only the ATWR distance estimation. Bottom: Zoom on the sensor node and the UAV. The complete hardware setup of the Wireless Sensor Node is shown top right.

the WUR receiver, reference in Fig. 8 labeled as *node in shutdown*. Approaching the targeted destination, the drone needs to send wake up beacons (Fig. 8 WUR TX) using the PIC in the 868 MHz band. These packets are streamed starting from the maximum UWB range, 100 m, which aims to enable the ATWR inside the safety range $\hat{d}$. Immediately after, the DW1000 on the drone sends the Blink message (Fig. 8) to check if the equivalent component on the sensor side is ready. Once the WUR beacon is received, the WUR module enables the MCU, which configures the UWB transceiver in a period equal to t_{init} (Fig. 8). At the next Blink transmission, the sensor node will correctly start the ATWR ranging protocol (Fig. 8), allowing the drone to precisely land at the WPT receive coil. Considering the path loss calculation shown in Fig. 4, we suppose that the WUR beacon is received on average between 10 m and 40 m, by ensuring the proper functioning of the UAV control algorithm during the last κ meters. On the other hand, the later the drone reawakens the wireless sensor node, this further reduces the ATWR energy usage. The maximum limit in which the UWB localization is necessary is within the κ radius, thus the drone can send the WUR beacon exactly $t_{beacon} + t_{init}$ seconds before entering the κ flight area.

6. Experimental evaluation

6.1. Test setup

The following experiments consider a UAV reaching the supposed PEB position from a distance beyond 100 m, above the UWB and WUR maximum coverage, and an *a priori* unknown angle of approach. Since our work aims to propose a low power but precise localization system for UAV combined with battery supplied sensor nodes, methodology assessment is based on the PEB idle-listening average power, in watts, and the multi-stage localization architecture energy usage, in joules. Table 2 provides an overview of test configurations and the technology used in each section. Much of our experimental work was conducted in

Table 2
Experimental Setup.

Section	Configuration	Test goals
Section 6.2	LPL + ATWR	Idle power; UAV approach energy
Section 6.3	WUR	WUR range and sensitivity
Section 6.4	WUR + ATWR	Idle power; UAV approach energy

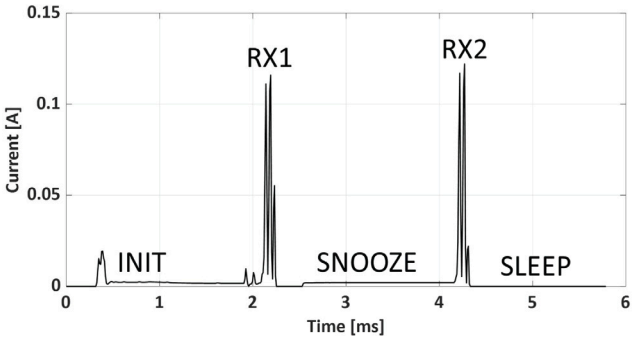

Fig. 10. Measured current consumption of the DW1000 low power listening mechanism.

a real environment at Richmond Park near London, United Kingdom. This area offers large expanses of open space, often characterized by strong winds; i.e. a perfect environment in which to test the reliability of our framework. Taking into consideration Eqs. (1), (2), and (3), we can estimate the average landing time given the drone's approaching speed $|v|$. In this example, we set up $|v|$ to 2 m/s. Between November and February, we performed 67 tests to fine-tune and characterize the UAV control algorithm and the ATWR protocol. In Fig. 13, the real-time speed and distance are shown. We acquired these values using the internal inertial module of the drone and the point-to-point distance with the sensor node, which is the relative reference point. Fig. 9 shows the complete Wireless Sensor Node and the test setup used to evaluate LPL and WUR performance. In a real environment, the UAV needs to change direction many times to correct for the effects of the lateral force of the wind. This effect is further increased during the final meters of the approach, where the speed is reduced and the propellers rotate more slowly, making it more difficult to combat the wind.

6.2. Low power listening and ATWR

To test the UWB low power listening capabilities, we programmed the DW1000 with the settings described in Section 5.3 at 1% DC. In Fig. 10, we show the measured current consumption of the low power listening mechanism previously explained (see Fig. 7). As expected, the measured peak current is 120 mA during RX widows, resulting in an average power consumption of 18.7 mW during the 4.02 ms LPL period. The average power in low power listening mode is equal to 190 μW with the 1% duty cycle setting.

As well as the LPL, we measured the average power consumption of the ATWR resulting in a continuous 400 mW, which heavily affects the overall battery life. Indeed, for the sake of comparison, audio sampling at 16 ksps needs 26 mW.

6.3. WUR

We performed a quantitative analysis of the performance of the WUR receiver in terms of range and sensitivity. We mounted the WUR transmitter and configured the transceiver to continuously send a 16-bit OOK address every 30 ms with transmit power set to 14 dBm. The WUR receiver, which was placed on the ground, was programmed so that whenever a message is detected, it lights an LED for one second. In our range evaluation experiment, the drone firstly flies far outside

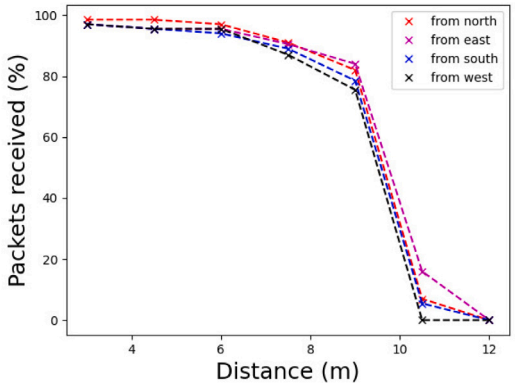

Fig. 11. WUR packet delivery ratio varying the distance and the angle of arrival. The drone is placed 2 m above ground.

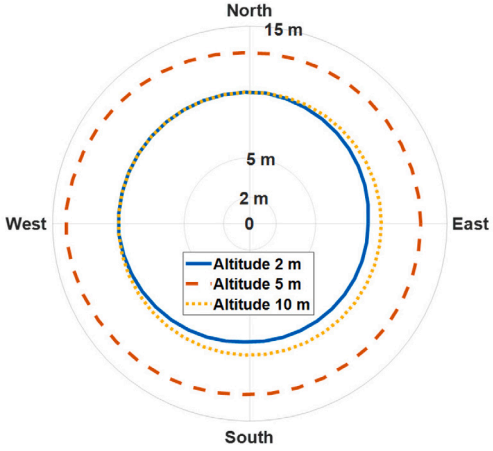

Fig. 12. Threshold distance for 80% packet delivery by varying the drone altitude and approaching angle. All units are in meters.

of the WUR range. The drone then starts approaching the sensor node point (thus the WUR receiver location) from four different directions, as presented in Fig. 11. We analyze the WUR range by observing the drone-WUR reported distance at the moment when the WUR led turns on. Both receiver and transmitter are equipped with a −2.3 dBi SMA antenna. We repeated this procedure 40 times, measuring a maximum communication distance of 15 m. This result is consistent with Fig. 4 in which we estimate a communication range between 10 m to 17 m using Earth Loss models. Due to the moving parts and the reflected waves generated in real environments, the packet loss cannot be disregarded; hence we measured it at varying planar distance, by setting the flight altitude at 2 m. Between 0 to 10 m, the wake up probability is above 90% with static objects, and above 80% during the flight (Fig. 11). Beyond the 10 meters threshold the link quality decreases. At 10 meters the packet loss is 80%, which further increases to 90% at 12 m. To verify the WUR behavior by varying the altitude, we checked the planar distance with respect to 80% packet delivery threshold at two different ground distances, 2 m and 5 m. Fig. 12 summarizes the results, which show an increased operability at 5 m. This comes from the antenna radiation pattern and the earth reflection losses that heavily affects the OOK modulation. With an altitude of 5 m, the WUR coverage gains between three to four meters, and for this reason it is preferable at κ radius.

These results fully support the asynchronous ranging protocol (Fig. 8) providing high reliability within 10 m range. To perform a sensitivity evaluation, we used the same transmitter, but we connected it to the WUR receiver through an adjustable RF attenuator. We

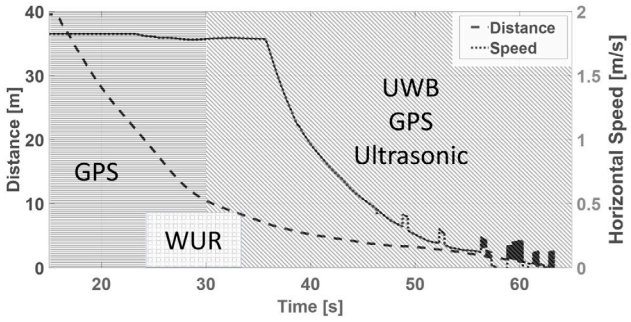

Fig. 13. Real landing path of the UAV with ATWR and WUR. Distance and speed are the scalar values measured from the 3 axes inertial module of the drone. Wind up to 5 m/s.

programmed the transmitter to send an OOK message in the same way as in the previous experiment, and we set the transmit power to 0 dBm. We connected a logic analyzer to the wake-up pin of the WUR. This pin gives a 1 ms pulse when the correct wake-up message is detected. As we increased the attenuation, we observed that below −45 dBm more than 10 % of the messages are lost.

The measured current consumption of the WUR module is 716 nA at 3.3 V, a value that must be added with the STM32WB55RG sleep current, which is 2.45 µA with the RTC active. However, the MCU current is equal for both implementations; hence it is not taken into consideration for further comparison with the duty-cycled approach.

6.4. LPL and WUR: in-field comparison

In our experiments, at 2 m/s, the overall precision landing procedure requires in average ∼71 s, where the last κ meters need 26 s. Indeed, the UAV control algorithm gradually decreases the velocity to avoid landing overshoot.

In the worst case, in terms of power consumption, the LPL setup can be woken up at the first receive window (Fig. 7 - RX1). For the whole landing approach, the sensor node needs 28.8 J for the LPL implementation without the WUR asynchronous wake up.

Due to the high reliability of the WUR transmission within 10 meters range from the targeted position, the UAV can send the OOK beacon at the edge of the κ circumference. The minimum distance in which is possible to send the WUR beacon is calculated as follows: with reference to Fig. 8, the procedure consists of two WUR beacons and one Blink packet. Eq. (5) provides the overall time (t_{min}), which is 78 ms in our setup.

$$t_{min} = 2t_{beacon} + P_{beacon} \tag{5}$$

At the $|v|$ speed limit, the drone covers approximately 16 cm, enabling the ATWR protocol only when it is really needed. In Fig. 14, the power consumption profile of the sensor board is plotted. The initial current spike highlights the WUR receiver operation, which does not correctly decode the beacon at the first attempt. After 30 ms a new beacon is received, and successfully decoded. Hence, the WUR circuit wakes up the STM32, which, after an initial configuration time, starts the ATWR ranging protocol. With this approach, the energy used by the sensor node to support the precision landing of the UAV is halved, enabling the expensive UWB protocol only for the last κ meters. On average, within a period of 26 s, the measured energy is 11 J, 2.6× less than the LPL approach.

Due to the GPS error, the UAV enabled the WUR transmitter at 20 m taking ∼40 s for the landing process (Fig. 13). In this case study, the sensor node used 16 J, 1.4× more than planned. However, while this result was collected in a challenging environment, is still 55% of the LPL approach (28.8 J in worst conditions), demonstrating the effective

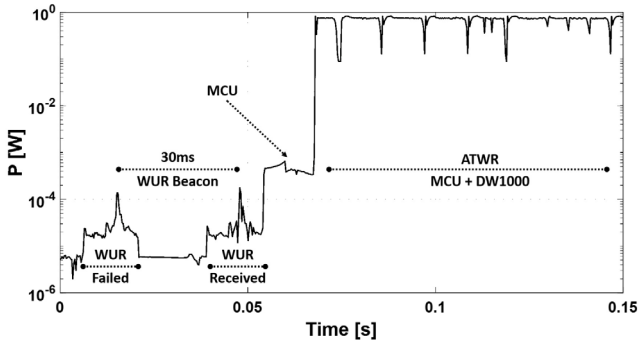

Fig. 14. Power consumption profile of the sensor node. In this specific case, the first received WUR beacon was corrupted, and the receiver discarded the wake up sequence.

Table 3
Results comparison between the low power listening (LPL) and the asynchronous wake up radio (WUR)

Section	Configuration	Sleep power [μW]	Landing energy [J]
Section 6.2	LPL + ATWR	190	29
Section 6.4	WUR + ATWR	2	11

reduction both for the landing energy and the sleep power used by the sensor node.

Upon completion of the landing stage, measurements acquired during the sensor activity are uploaded to the drone at the high data rate used by *Configuration 2*. In this condition, we verified the real throughput of the payload, which should be maximized in order to minimize the total interaction time between the UAV and the sensor. During data transfer, the DW1000 can sustain a real bit-rate of 5.988 Mbps with a packet size of 1 kB, and 4.932 Mbps respectively with 700 B. Using packets smaller than 500 B drastically reduces the average performance, which reach a maximum of 1 Mbps. Final results show that the DW1000 needs 43 s to upload the entire contents of the local storage (256 MB).

7. Conclusion

This paper presents a new open platform to enable efficient localization for wireless data and power transfer between drones and static wireless sensor devices. Fusing GPS and UWB distance estimation, precision landing within 20 cm error is achieved. We experimentally verified the effective throughput of the DW1000 in *Configuration 2*, which reaches a continuous speed of 6 Mbps. We examine both low power listening UWB and wake-up radio approaches, providing models and measurements to estimate power consumption in non-ranging states and during the drone's approach phase. We demonstrated both solutions with accurate in field-test comparisons, achieving an energy reduction up to 62% using the WUR approach, which deviates to ∼50% in challenging windy conditions. In these conditions, the WUR performance fully supports the precision landing required, with a packet delivery ratio above 80% within 10 m range and a maximum latency of 30 ms. In our experiments, the maximum coverage is achieved between 2 m and 5 m altitude, at which the drone should fly during wake-up triggering to maximize the system reliability. The raw data from the field experiments reported in this work will be made publicly available on GitHub. They demonstrate the effectiveness of our framework, fusing the benefits of asynchronous WUR and UWB distance measurement. Finally, concerning the sleep current of the sensor node presented in Table 3, we show that the WUR solution reduces the average power up to 95×, or, with equal latency 1566×, with 1% and 17% DC in LPL mode, respectively. On the other hand, a duty cycle of 0.01% is required to reach an average power of 2 μW, giving a latency of 40 s.

CRediT authorship contribution statement

Tommaso Polonelli: Methodology, Formal analysis, Visualization, Original draft preparation. **Michele Magno:** Conceptualization, Reviewing. **Vlad Niculescu:** Software, Visualization. **Luca Benini:** Supervision, Writing – review & editing. **David Boyle:** Conceptualization, Supervision, Writing – review & editing.

Declaration of competing interest

The authors declare that they have no known competing financial interests or personal relationships that could have appeared to influence the work reported in this paper.

References

[1] Business Insider, Commercial unmanned aerial vehicle (UAV) market analysis – industry trends, forecasts and companies, 2020, https://www.businessinsider.com/commercial-uav-market-analysis, (accessed July 9, 2020).
[2] Goldman Sachs, DRONES reporting for work, 2020, https://www.goldmansachs.com/insights/technology-driving-innovation/drones/, (accessed July 9, 2020).
[3] A. Dhekne, A. Chakraborty, K. Sundaresan, S. Rangarajan, TrackIO: tracking first responders inside-out, in: 16th {USENIX} Symposium on Networked Systems Design and Implementation ({NSDI} 19), 2019, pp. 751–764.
[4] A. Boubrima, E.W. Knightly, Robust mission planning of UAV networks for environmental sensing, in: DroNet@ MobiSys, 2020, 2–1.
[5] M. Dunbabin, P. Corke, I. Vasilescu, D. Rus, Data muling over underwater wireless sensor networks using an autonomous underwater vehicle, in: Proceedings 2006 IEEE International Conference on Robotics and Automation, 2006. ICRA 2006. 2006, pp. 2091–2098.
[6] O. Tekdas, V. Isler, J.H. Lim, A. Terzis, Using mobile robots to harvest data from sensor fields, IEEE Wirel. Commun. 16 (1) (2009) 22–28.
[7] D. Popescu, C. Dragana, F. Stoican, L. Ichim, G. Stamatescu, A collaborative UAV-WSN network for monitoring large areas, Sensors 18 (12) (2018) 4202.
[8] Y. Qin, D. Boyle, E. Yeatman, Efficient and reliable aerial communication with wireless sensors, IEEE Internet Things J. 6 (5) (2019) 9000–9011.
[9] A. Kurs, A. Karalis, R. Moffatt, J.D. Joannopoulos, P. Fisher, M. Soljačić, Wireless power transfer via strongly coupled magnetic resonances, Science 317 (5834) (2007) 83–86, http://dx.doi.org/10.1126/science.1143254.
[10] D.E. Boyle, M.E. Kiziroglou, P.D. Mitcheson, E.M. Yeatman, Energy provision and storage for pervasive computing, IEEE Pervasive Comput. 15 (4) (2016) 28–35.
[11] P.D. Mitcheson, D. Boyle, G. Kkelis, D. Yates, J.A. Saenz, S. Aldhaher, E. Yeatman, Energy-autonomous sensing systems using drones, in: 2017 IEEE SENSORS, 2017, pp. 1–3.
[12] M. Ballerini, T. Polonelli, D. Brunelli, M. Magno, L. Benini, Experimental evaluation on NB-IoT and LoRaWAN for industrial and IoT applications, in: 2019 IEEE 17th International Conference on Industrial Informatics (INDIN), 1, IEEE, 2019, pp. 1729–1732.
[13] D. Zorbas, C. Douligeris, Computing optimal drone positions to wirelessly recharge IoT devices, in: IEEE INFOCOM 2018 - IEEE Conference on Computer Communications Workshops (INFOCOM WKSHPS), 2018, pp. 628–633.
[14] A. Ledergerber, R. D'Andrea, Ultra-wideband range measurement model with Gaussian processes, in: 2017 IEEE Conference on Control Technology and Applications (CCTA), IEEE, 2017, pp. 1929–1934.
[15] P. Mayer, M. Magno, C. Schnetzler, L. Benini, EmbedUWB: Low power embedded high-precision and low latency UWB localization, in: 2019 IEEE 5th World Forum on Internet of Things (WF-IoT), IEEE, 2019, pp. 519–523.
[16] Y. Qin, D. Boyle, E. Yeatman, Radio diversity for heterogeneous communication with wireless sensors, in: 2019 IEEE 5th World Forum on Internet of Things (WF-IoT), IEEE, 2019, pp. 955–960.
[17] O. Briante, A.M. Mandalari, A. Molinaro, G. Ruggeri, J. Alonso-Zarate, F. Vazquez-Gallego, Duty-cycle optimization for machine-to-machine area networks based on frame slotted-ALOHA with energy harvesting capabilities, in: European Wireless 2014; 20th European Wireless Conference, VDE, 2014, pp. 1–6.
[18] D. Boyle, R. Kolcun, E. Yeatman, Energy-efficient communication in wireless networks, in: ICT-Energy Concepts for Energy Efficiency and Sustainability, InTech, 2017.
[19] M. Magno, V. Jelicic, B. Srbinovski, V. Bilas, E. Popovici, L. Benini, Design, implementation, and performance evaluation of a flexible low-latency nanowatt wake-up radio receiver, IEEE Trans. Ind. Inf. 12 (2) (2016) 633–644.
[20] L. Gupta, R. Jain, G. Vaszkun, Survey of important issues in UAV communication networks, IEEE Commun. Surv. Tutor. 18 (2) (2015) 1123–1152.
[21] J. Tiemann, C. Wietfeld, Scalable and precise multi-UAV indoor navigation using TDOA-based UWB localization, in: 2017 International Conference on Indoor Positioning and Indoor Navigation (IPIN), IEEE, 2017, pp. 1–7.

[22] P. Corbalán, G.P. Picco, Concurrent ranging in ultra-wideband radios: Experimental evidence, challenges, and opportunities., in: EWSN, 2018, pp. 55–66.
[23] IEEE802, DW1000, 15.4-2011 UWB Transceiver, Datasheet, Decawave, 2016.
[24] C. Budaciu, N. Botezatu, M. Kloetzer, A. Burlacu, On the evaluation of the crazyflie modular quadcopter system, in: 2019 24th IEEE International Conference on Emerging Technologies and Factory Automation (ETFA), IEEE, 2019, pp. 1189–1195.
[25] K. Ashhar, C.B. Soh, K.H. Kong, Wireless ultrawideband sensor network for gait analysis in rehabilitation clinics, in: 2018 IEEE International Conference on Systems, Man, and Cybernetics (SMC), IEEE, 2018, pp. 1524–1529.
[26] Y.H. Shin, S. Lee, J. Seo, Autonomous safe landing-area determination for rotorcraft UAVs using multiple IR-UWB radars, Aerosp. Sci. Technol. 69 (2017) 617–624.
[27] T. Polonelli, M. Magno, L. Benini, An ultra-low power wake up radio with addressing and retransmission capabilities for advanced energy efficient MAC protocols, in: 2016 15th ACM/IEEE International Conference on Information Processing in Sensor Networks (IPSN), IEEE, 2016, pp. 1–2.
[28] N.E. Roberts, D.D. Wentzloff, A 98nW wake-up radio for wireless body area networks, in: 2012 IEEE Radio Frequency Integrated Circuits Symposium, IEEE, 2012, pp. 373–376.
[29] P. Le-Huy, S. Roy, Low-power wake-up radio for wireless sensor networks, Mob. Netw. Appl. 15 (2) (2010) 226–236.
[30] R. Piyare, A.L. Murphy, C. Kiraly, P. Tosato, D. Brunelli, Ultra low power wake-up radios: A hardware and networking survey, IEEE Commun. Surv. Tutor. 19 (4) (2017) 2117–2157.
[31] D. Spenza, M. Magno, S. Basagni, L. Benini, M. Paoli, C. Petrioli, Beyond duty cycling: Wake-up radio with selective awakenings for long-lived wireless sensing systems, in: 2015 IEEE Conference on Computer Communications (INFOCOM), IEEE, 2015, pp. 522–530.
[32] H. Karvonen, J. Iinatti, J. Petäjäjärvi, M. Hämäläinen, Energy efficient IR-UWB WBAN using a generic wake-up radio based MAC protocol, in: Proceedings of the 9th International Conference on Body Area Networks, 2014, pp. 358–364.
[33] S. Aldhaher, P.D. Mitcheson, J.M. Arteaga, G. Kkelis, D.C. Yates, Light-weight wireless power transfer for mid-air charging of drones, in: 2017 11th European Conference on Antennas and Propagation (EUCAP), IEEE, 2017, pp. 336–340.
[34] J.M. Arteaga, L. Lan, S. Aldhaher, G. Kkelis, D.C. Yates, P.D. Mitcheson, A multi-MHz IPT-link developed for load characterisation at highly variable coupling factor, in: 2018 IEEE Wireless Power Transfer Conference (WPTC), IEEE, 2018, pp. 1–4.
[35] A. Pandiyan, D. Boyle, M. Kiziroglou, S. Wright, E. Yeatman, Optimal dynamic recharge scheduling for two stage wireless power transfer, IEEE Trans. Ind. Inf. (2020) 1.
[36] P. Chermprayong, K. Zhang, F. Xiao, M. Kovac, An Integrated Delta manipulator for aerial repair: A new aerial robotic system, IEEE Robot. Autom. Mag. 26 (1) (2019) 54–66.
[37] P. Corbalán, G.P. Picco, Ultra-wideband concurrent ranging, 2020, arXiv preprint arXiv:2004.06324.
[38] D. Hoeller, A. Ledergerber, M. Hamer, R. D'Andrea, Augmenting ultra-wideband localization with computer vision for accurate flight, IFAC-PapersOnLine 50 (1) (2017) 12734–12740, 20th IFAC World Congress.
[39] O.J. Faqir, E.C. Kerrigan, D. Gündüz, Joint optimization of transmission and propulsion in aerial communication networks, in: 2017 IEEE 56th Annual Conference on Decision and Control (CDC), IEEE, 2017, pp. 3955–3960.
[40] R.C. Carrano, D. Passos, L.C. Magalhaes, C.V. Albuquerque, Survey and taxonomy of duty cycling mechanisms in wireless sensor networks, IEEE Commun. Surv. Tutor. 16 (1) (2013) 181–194.
[41] M. Del Prete, A. Costanzo, D. Masotti, T. Polonelli, M. Magno, L. Benini, Experimental analysis of power optimized waveforms for enhancing wake-up radio sensitivity, in: 2016 IEEE MTT-S International Microwave Symposium (IMS), IEEE, 2016, pp. 1–4.
[42] Infineon, RF and microwave power detection with schottky diodes, version X.Y, 2018, URL: http://tiny.cc/o1thlz.
[43] DW1000 User Manual, Version, 2.11.(DecaWave, 2017), 2019.
[44] M. Malajner, P. Planinšič, D. Gleich, UWB ranging accuracy, in: 2015 International Conference on Systems, Signals and Image Processing (IWSSIP), IEEE, 2015, pp. 61–64.
[45] DecaWave, ASP013: The implementation of two-way ranging with the DW1000, Decawave Limited, 2015.